Study of structural and electrical properties of Zn-doped barium titanate ceramics synthesized by conventional solid-state method

EHSAN UL HAQ[1], MUHAMMAD RAMZAN ABDUL KARIM[2,*], KHURRAM IMRAN KHAN[2,*],
WASEEM AKRAM[1], SYED SHABBAR HASSAN[1], FAHAD KASHIF[1]
[1]*Department of Metallurgical and Materials Engineering, University of Engineering and Technology, Lahore-54890, Pakistan*
[2]*Faculty of Materials and Chemical Engineering, GIK Institute of Engineering Sciences and Technology, Topi-23640, Pakistan*

Barium Titanate ($BaTiO_3$) is a prominent ceramic material with piezoelectric and ferroelectric properties. Despite having the wide range of applications in actuators, optoelectronics and capacitors, the high response time and dielectric losses in $BaTiO_3$ limit its efficient utilization. Zinc oxide (ZnO) has been a dopant of choice in several studies for controlling grain growth behavior and dielectric properties of piezoelectric materials. In this study, various ZnO concentrations ranging from 0.02 wt.% to 0.08 wt.% were added in barium titanate ($BaTiO_3$) through conventional solid-state method followed by sintering at 1150 °C for 2 hours. In X-ray diffraction (XRD) analysis, no secondary phase has been detected for all dopant concentrations showing that all ZnO added had been incorporated in $BaTiO_3$ to form the solid solution with chemical formulation of $BaZn_xTi_{1-x}O_3$. The complex impedance spectroscopy (CIS) showed that the highest dipolar and interfacial polarization/ capacitance of more than 50 F was exhibited by 0.06 wt. % ZnO doped $BaTiO_3$. This composition is ideal for capacitive applications particularly at frequencies above 1000KHz.

(Received September 30, 2019; accepted February 11, 2022)

Keywords: Barium titanate, Electrical properties, Dielectrics, Structural analysis, Impedance spectroscopy

1. Introduction

Attention to metal oxides due to their unique properties as well as efficiency in various fields of science has grown significantly in recent years [1–3]. Among the various metal oxides, barium titanate is considered a pioneer ceramic in the history of advanced materials since 1945 [4,5]. In this era of advancing technologies especially in the electro ceramics and microelectronics, there is need to produce advanced ceramics with ultra-high purity and excellent properties like less response time and fast operation as required for sensors, actuators, motors, and transducers etc. Barium titanate ($BaTiO_3$) is a fascinating material in this context due to its ferro-electric and piezo-electric behavior [5]. Various studies have been done to improve and modify the properties of barium titanates and its derivates by adding in it various dopants e.g. Mn [6–8], Sr [9], Zr [10], Ca [11], Ce [12,13], Fe and Nb [14,15], Mg [16], Ni [17], Tb [18] Gd^{+3} [19], La [20] nano carbon black [21], various other transition metals [22] and even polymer composites of $BaTiO_3$ have been made for this purpose [23,24]. Zn has also been used as dopant in $BaTiO_3$ with different processing techniques like laser deposition [25] and sol gel processing [26-29]. $BaTiO_3$ belongs to perovskite (ABO_3) family of crystal structures having Ba^{+2} ions incorporated at corners (A-site), O^{-2} ions at faces and Ti^{+4} ion present at body centered position (B-site); in actual slightly shifted. This shift in titanium ion induces inherent polarization in $BaTiO_3$ that makes it ferro-electric and dielectric material [5]. Due to its capacitive and piezoelectric properties it is being used in wide range of applications including capacitors [30], actuators, transducers multilayer ceramic capacitor, PTC–thermistors, piezoelectric transducers [31-33], sensors [34-37], dynamic RAM, MEMS, optical modulators, electromechanical devices etc. [38–40]. ZnO-doping has been reported in numerous studies with major interest in it owing to its grain-controlling behavior, improved densification during sintering, and capability to enhance permittivity and dielectric properties of $BaTiO_3$ by lowering the dielectric losses [4,41,42]. ZnO, therefore, has been used in present work with concentrations range of 0.02-0.08 wt.% to allow least distortion in the perovskite phase of tetragonal symmetry thus retaining the space group P4mm while minimizing the dielectric losses. XRD confirmed the formation of desired material whereas impedance spectroscopy (IR) evaluated the electrical properties. Purpose of this work was to study the effect of ZnO doping on lattice parameters and electrical properties including resistance, capacitance, and conductance and dielectric losses of $BaTiO_3$. This work will help producers in manufacturing of products with enhanced electrical properties.

2. Experimental procedure

In this work a conventional solid-state technique has been used to synthesize Zn doped $BaTiO_3$. Stoichiometric calculations were done by unitary method to find the respective weights of $BaCO_3$, TiO_2 and ZnO to produce $BaZn_xTi_{1-x}O_3$, where x = 0.02, 0.04, 0.06 and 0.08. Zn-doped barium titanate will be abbreviated as ZBT in this work. Raw materials were weighed using electric balance separately for each value of x to produce 10 grams of $BaZn_xTi_{1-x}O_3$. Mixing and milling of ingredients placed in teflon pots was done in planetary ball mill by using methanol solvent at 170 rpm for 30 minutes. Yitria stabilized zirconia (YSZ) balls of different sizes were used as grinding media. Drying of milled mixture was done in oven at 120 ^{0}C to remove the solvent. For approximation of calcination temperature, TGA/DTA technique was used in which dry powdered samples of $BaZn_xTi_{1-x}O_3$ were heated from 40-1000 ^{o}C at the rate of 50 ^{o}C/min, then soaked at 1000 ^{o}C for 300 seconds and cooled down to 40 ^{o}C at the rate of 50 ^{o}C/min. The quick TGA/DTA scans gave calcination temperature range from 900-1150 ^{o}C. So, powder mixture was calcined in box furnace at 1150 ^{o}C for 1 hour. Then by using uniaxial hydraulic press, pellets of diameter 10 mm and thickness 1.5 mm were produced by applying load of 6000 lb. As the last step of processing, sintering of all pellets, having different dopant concentrations, was done in box furnace at 1150 ^{o}C for 2 hours. After sintering of pellets their density measurement was done using pycnometer. Then characterization of these pellets was done using XRD in which crystal structure was studied. The 1900 QuadTech Precision LCR meter was used to perform complex impedance spectroscopy (CIS) of the respective compositions by silver-coating the ZBT pellets to finally characterize them for the capacitive/dielectric properties. The cole-cole plots (Fig. 4) were generated with the frequency 100Hz-1MHz on X-axis and impedance on Y-axis to compare the electrical properties as a function of varying dopant-concentration. The tan delta (tan δ) is proportional to dielectric loss given as a function of frequency in Fig. 3.

3. Results

Diffraction patterns of $BaZn_xTi_{1-x}O_3$ having Zn concentration in the order of x=0, 0.02, 0.04, 0.06 ,0.08 wt. %, confirm the presence of mono-phasic $BaTiO_3$. The XRD peaks shown in Fig. 1 (left) match with peaks of pure $BaTiO_3$ as per ICDD (International Card for Diffraction Data) PDF no. 05-0626.

XRD patterns show right shift in the diffiraction peaks with the increase in x values as shown in Fig. 1 (right), which means a decrease in inter planar spacing. Consequently lattice constants determined from d-spacing show decrease in values with increase in dopant concentration as shown in Table 1.

Table 1. Lattice constant and Volume of ZnO doped $BaTiO_3$ with the tetragonal symmetry and P4mm space group

wt.% ZnO doped in $BaTiO_3$	a=b (A^0)	c (A^0)	c/a	Vol $(A^0)^3$
0 (Pure $BaTiO_3$)	3.997	4.027	1.007	64.364
0.02	3.994	4.026	1.008	64.243
0.04	3.991	4.025	1.008	64.108
0.06	3.987	4.024	1.009	63.969
0.08	3.983	4.023	1.009	63.839

Complex impedance spectroscopy was used to analyze the effect of dopant on conductance, resistance, dielectric loss, relaxation time and impedance was determined. Capacitance showed variation in trend for all dopant concentration shown in Fig. 2 (left). Capacitance is decreased by increasing frequency for all dopant concentrations. Maximum capacitance was shown by ZBT having x = 0.06 wt. % ZnO at all frequencies. Whereas x = 0.08 wt. % ZnO showed minimum capacitance at low frequencies but at high frequencies x = 0.04 wt. % ZnO ZBT behaved least capacitive. Resistance values showed variation in trend throughout the frequency range (1000 Hz to 1 MHz).

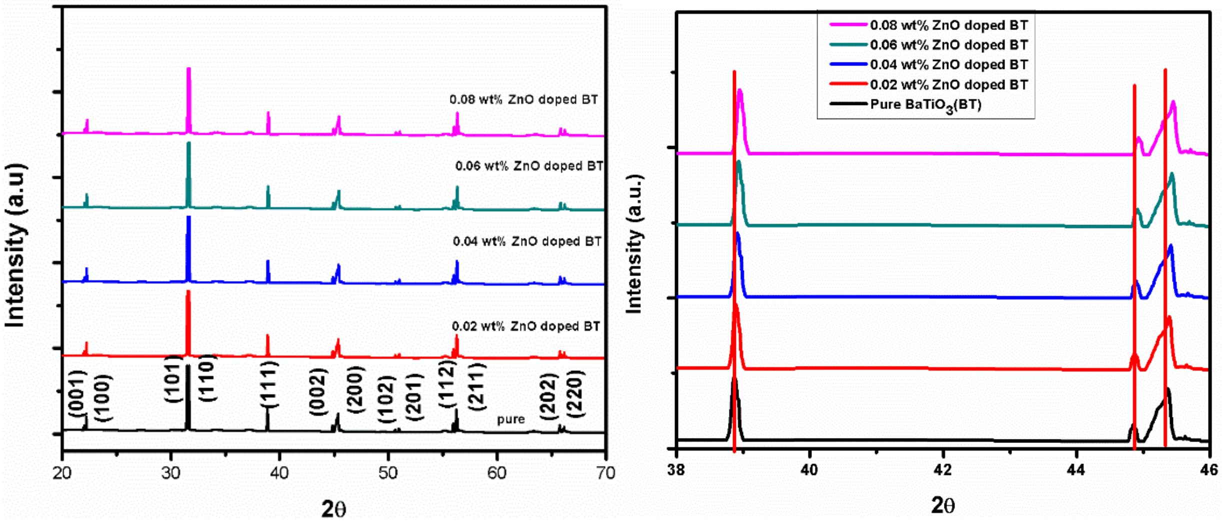

Fig. 1. Diffraction peaks as obtained from XRD data for ZnO doped barium titanate specimens (left), and representation of peak shifting towards right as a function of wt. % of ZnO (right) (color online)

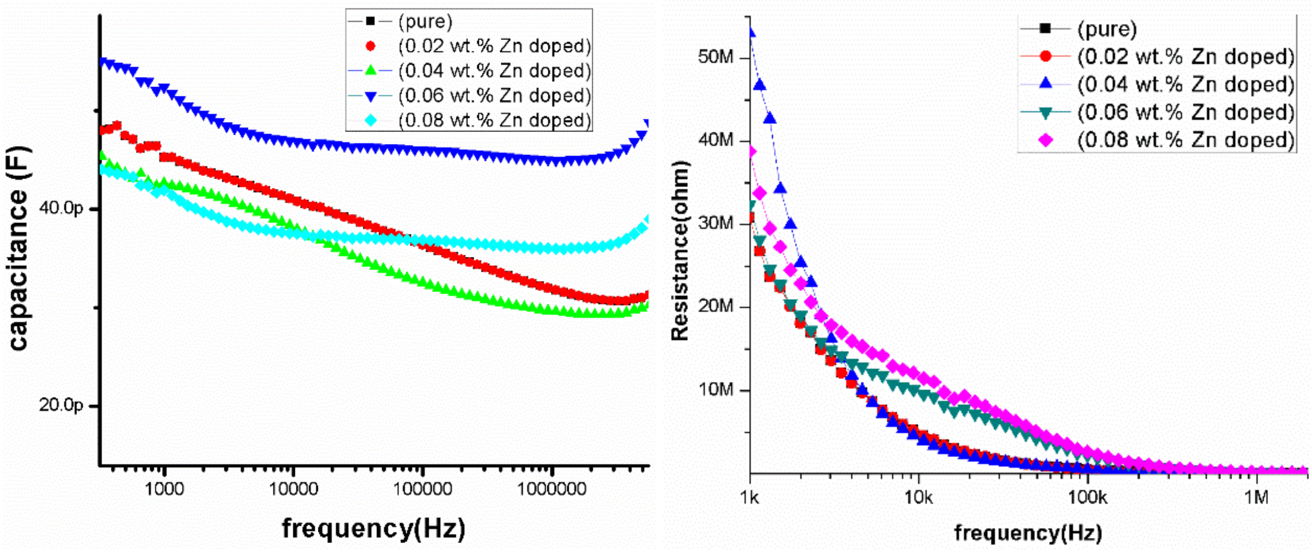

Fig. 2. Relationship between capacitance and frequency (left), resistance and frequency (right) for un-doped barium titanate (BT) and Zn doped barium titanate (ZBT) at various concentrations of dopant (x = 0.02, 0.04, 0.06, 0.08 wt.%) (color online)

For all values of x with increasing frequency, the resistance of ZBT decreases as shown in Fig. 2 (right). ZBT with x = 0.04 show highest resistance at lower frequencies but at high frequencies it has least resistance. Conductance of ZBT exhibited no marked variation at lower frequencies but increased at higher frequencies as shown in Fig. 3 (left). However, this increase in conductance is more prominent for low ZnO concentrations as compared with higher concentrations. Dielectric loss for x= 0.04 wt. % ZnO is minimum at lower frequencies but at 23133.5 Hz, it showed highest value then again fall in curve took place as shown in Fig. 3 (right). Unlike x = 0.04, all other compositions showed decrease in dielectric loss with increasing x as well as frequency values.

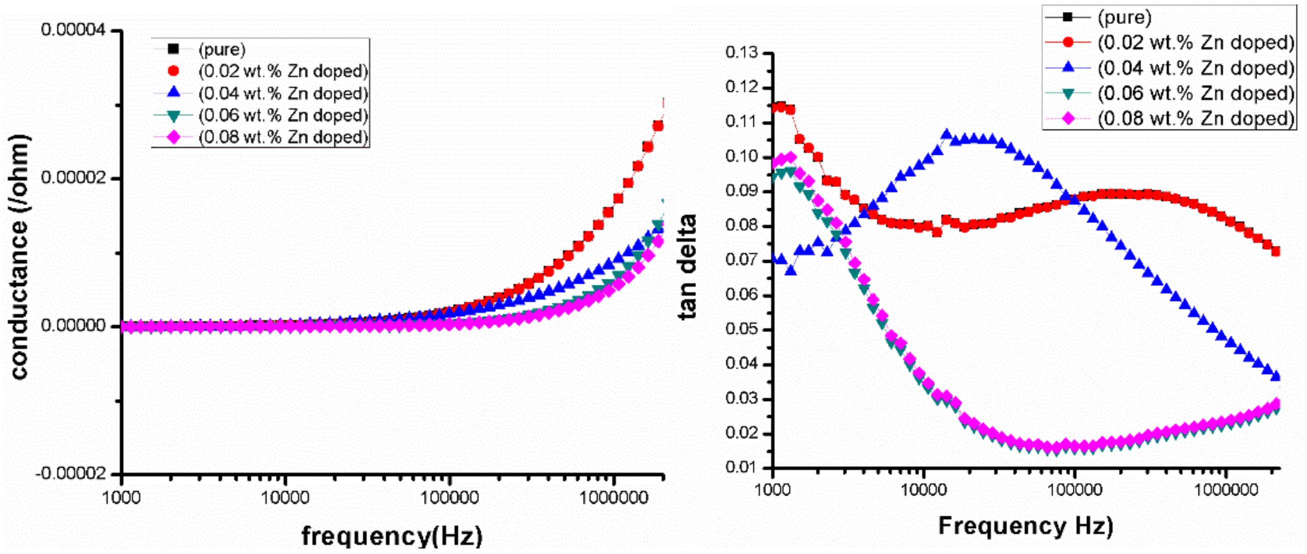

Fig. 3. Plots between conductance and frequency (left) and dielectric loss and frequency (right) for un-doped barium titanate (BT) and Zn doped barium titanate (ZBT) at various concentrations of dopant (x = 0.02, 0.04, 0.06, 0.08 wt.%) (color online)

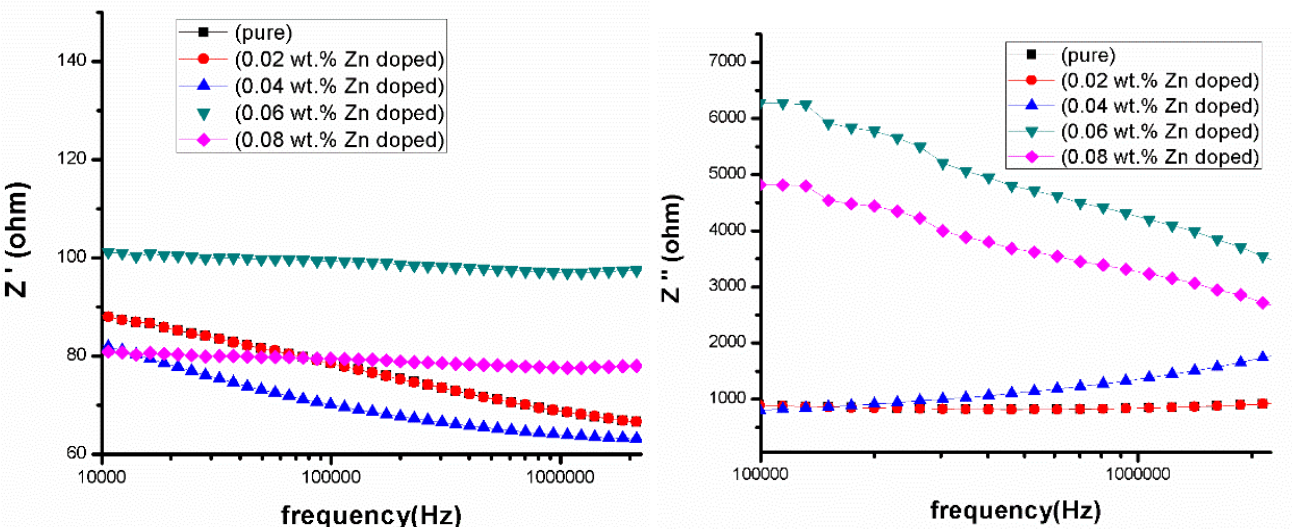

Fig. 4. Plots between real part of impedance Z' and frequency (left) and, Imaginary part of impedance Z" and frequency (right) for un-doped barium titanate (BT) and Zn doped barium titanate (ZBT) (color online)

Fig. 4 (left) shows that plot of frequency vs real part of impedance (Z`) exhibits varying trend with increasing x in ZBT. At x = 0.06, ZBT has maximum value of Z` whereas at x = 0.04, it has lowest values. Remarkable decrease in Z` value with increasing frequency is shown by x = 0, 0.02, 0.04 BZT. Imaginary part of impedance (Z") vs frequency plot as shown in Fig. 4 (right) described the descending trend of the x = 0.06, 0.08 while ascending trend of x = 0.04 unlike un-doped and 0.02 ZBT having straight graph with increasing frequency.

4. Discussion

It is obvious interpretation from analysis of XRD plots that no secondary phase was detected in all dopant concentrations and whole amount of ZnO added had been incorporated in $BaTiO_3$ to form solid solution with chemical formulation of $BaZn_xTi_{1-x}O_3$ where x=0.02,0.04,0.06,0.08 as it can be comprehended in Fig. 1 (left). But zoomed view of XRD plots in Fig. 1 (right), showed a noticeable peak shifting of doped compositions rightwards as compared to pure $BaTiO_3$. To satisfy Bragg's equation, as 2 theta increases, inter-planer spacing (d-spacing) must decrease and resultantly lattice parameters showed decreased values too. The structural reasoning behind this decrease in lattice parameters is the fact that Zn^{+2} substitutes Ba^{+2} (Zn^{+2} = 74pm and Ba^{+2} = 135pm) at A site irrespective of Shannon ionic radii to satisfy charge neutrality obeying Vegard's law [43]. Also increase in c/a ratio shows that distortion in "c" length is greater than that in "a" length. Due to larger cation, lattice parameters showed smaller values as demonstrated in Table 1.

As for the electrical properties, it can be seen from Fig. 2 (left), that capacitance is highest for ZBT with x=0.06 so it is suitable for applications in capacitors especially at higher frequencies where other compositions show low capacitance. The composition with x=0.06 wt. % ZnO also showed the lowest conductance which ensures good dielectric properties as depicted by Fig. 3 (left). The value of Z' which is actually a measure of relative permittivity also showed high values in case of x=0.06 as shown in Fig. 4 (left). Dielectric loss is minimum for x=0.06 whereas higher for all other values. All the above-mentioned electrical properties are showing their values most desired for capacitive point of view at x=0.06. This is because ZBT is showing highest polarization at this dopant concentration, especially dipolar and interfacial polarization [38].

5. Conclusions

Zn doped $BaTiO_3$ (0.02-0.08 wt.% ZnO) has been prepared by conventional solid-state method. The XRD plots indicated tetragonal symmetry with P4mm space group. The shrinking lattice parameters with the increasing dopant concentration have been observed. Formation of A-site substituted $BaTiO_3$ has been confirmed by XRD as well. Importantly, no secondary phase was detected in all dopant concentrations indicating that the whole amount of ZnO added had been incorporated in $BaTiO_3$ to form solid solution with chemical formulation of $BaZn_xTi_{1-x}O_3$. The complex impedance spectroscopy (CIS) has shown that the best dielectric properties have been observed by doping Zn in $BaTiO_3$ with precursor (ZnO) concentration of 0.06 wt. %. At this composition, tan delta (tan δ), representing dielectric loss, was found to be the lowest 0.025 at 1000KHz. Moreover, the capacitance values of more than 50F across all the frequency range with such a low loss-tangent imply that these findings are promising for the development of highly capacitive piezoceramics.

References

[1] X. Yu, T.J. Marks, A. Facchetti: Nat. Mater. **15**, 383 (2016).

[2] P. Kumbhakar, C. Chowde Gowda, P. L. Mahapatra,

M. Mukherjee, K. D. Malviya, M. Chaker, A. Chandra, B. Lahiri, P. M. Ajayan, D. Jariwala, A. Singh, C. S. Tiwary, Mater. Today **45**, 142 (2021).

[3] W. Chen, X. Hou, X. Shi, H. Pan, ACS Appl. Mater. Interfaces **10**, 35289 (2018).

[4] Q. K. Muhammad, M. Waqar, M.A . Rafiq, M. N. Rafiq, M. Usman, M. S. Anwar, J. Mater. Sci., **51**, 10048 (2016).

[5] M. M. Vijatović, J. D. Bobić, B. D. Stojanović, Sci. Sinter. **40**, 235 (2008).

[6] Y. Shuai, S. Q. Zhou, H. Schmidt, Adv. Sci. Technol. **67**, 212 (2010).

[7] D. P. Norton, N. A. Theodoropoulou, A. F. Hebard, J. D. Budai, L. A. Boatner, S. J. Pearton, R. G. Wilson, Electrochem. Solid-State Lett. **6**, G19 (2003).

[8] X. Tong, Y.-H. Lin, S. Zhang, Y. Wang, C.-W. Nan, J. Appl. Phys. **104**, 066108 (2008).

[9] S. Uddin, S. Hameed, N. Ali, K. Althubeiti, A. Zaman, H. Alrobei, M. Mushtaq, A. Ali, F. Sultana, Mater. Res. Express **8**, 096101 (2021).

[10] B. Garbarz-Glos, K. Bormanis, D. Sitko, Ferroelectrics **417**, 118 (2011).

[11] S. Uddin, A. Zaman, I. Rasool, S. Akbar, M. Kamran, N. Mehboob, A. Ali, A. Ahmad, M. F. Nasir, Z. Iqbal, J. Ceram. Process. Res. **21**, 745 (2020).

[12] G. Confalonieri, V. Buscaglia, G. Canu, M. T. Buscaglia, M. Dapiaggi, J. Synchrotron Radiat. **26**, 1280 (2019).

[13] S. Yasmm, S. Choudhury, M. A. Hakim, A. H. Bhuiyan, M. J. Rahman, J. Mater. Sci. Technol. **27**, 759 (2011).

[14] G. P. Du, Z. J. Hu, Q. F. Han, X. M. Qin, W. Z. Shi, J. Alloys Compd. **492**, 79 (2010).

[15] F. Lin, W. Shi: J. Alloys Compd. **495**, 167 (2010).

[16] W. Cai, C. L. Fu, J. C. Gao, C. X. Zhao, Adv. Appl. Ceram. **110**, 181 (2011).

[17] S. K. Das, R. N. Mishra, B. K. Roul, Solid State Commun. **191**, 19 (2014).

[18] H. Lu, L. Liu, J. Lin, W. Yang, L. Weng, X. Zhang, Ceram. Int. **44**, 6514 (2018).

[19] J. P. Hernández Lara, M. Pérez Labra, F. R. Barrientos Hernández, J. A. Romero Serrano, E. O. Ávila Dávila, P. Thangarasu, A. Hernández Ramirez, Mater. Res. **20**, 538 (2017).

[20] V. Paunović, V. Mitić, M. Marjanović, L. Kocić, Facta Universitatis, Series: Electronics and Energetics **29**, 285 (2016).

[21] T. Seetawan, W. Photankham, H. Wattanasarn, S. Phewphong, Mater. Today Proc. **4**, 6472 (2017).

[22] F. Lin, W. Shi J. Alloys Compd. **475**, 64 (2009).

[23] J. Su, J. Zhang, J. Mater. Sci. Mater. Electron. **27**, 4344 (2016).

[24] S. Uddin, N. Akhtar, S. Bibi, A. Zaman, A. Ali, K. Althubeiti, H. Alrobei, M. Mushtaq, Mater. **14**, 5430 (2021).

[25] A. Y. Fasasi, M. Maaza, E. G. Rohwer, D. Knoessen, C. Theron, A. Leitch, U. Buttner, Thin Solid Films **516**, 6226 (2008).

[26] S. K. Das, R. N. Mishra, B. K. Roul, Solid State Commun. **191**, 19 (2014).

[27] X. Liu, X. Deng, K. Liu, W. Cai, C. Fu, Integr. Ferroelectr. **150**, 66 (2014).

[28] L. Gao, J. Zhai, X. Yao, Appl. Surf. Sci. **255**, 4521 (2009).

[29] L. P. Zhu, H. M. Deng, X. X. Li, L. Qian, H. Deng, L. Zhu, D. J. Huang, F. Chen, W. L. Gao, P. X. Yang, J. H. Chu, J. Phys. Conf. Ser. **276**, 12163 (2011).

[30] P. N. Nikolarakis, I. A. Asimakopoulos, L. Zoumpoulakis, J. Nanomater. **2018**, 1 (2018).

[31] R. Ul, R. Rouffaud, M. P. Thi, C. Bantignies, L. Tran-Huu-Hue, F. Levassort, in 2017 IEEE International Ultrasonics Symposium (IUS), 1 (2017).

[32] W. W. Willmarth, Rev. Sci. Instrum. **29**, 218 (1958).

[33] G. E. C. Ltd., J. Sci. Instrum. **33**, 287 (1956).

[34] J. Wang, H. Wan, Q. Lin, Meas. Sci. Technol. **14**, 172 (2003).

[35] S. Sharma, A. Sharma, M. Tomar, N. K. Puri, V. Gupta, Procedia Eng. **87**, 1067 (2014).

[36] M. Singh, B. C. Yadav, A. Ranjan, M. Kaur, S. K. Gupta, Sensors Actuators B Chem. **241**, 1170 (2017).

[37] K. Maeda, I. Fujii, K. Nakashima, G. Fujimoto, K. Suma, T. Sukigara, S. Wada, J. Ceram. Soc. Japan **121**, 698 (2013).

[38] N. Humera, H. Noor, S. Riaz, S. Naseem, Advances in Civil, Environmental, and Materials Research (ACEM16), Jeju Island, Korea, 2016.

[39] S. Ramakanth, S. Hamad, S. Venugopal Rao, K. C. James Raju, AIP Adv. **5**, 057139 (2015).

[40] A. Y. Tsivadze, G. V. Ionova, V. K. Mikhalko, I. S. Ionova, G. A. Gerasimova, Prot. Met. Phys. Chem. Surfaces **52**, 61 (2016).

[41] X. Liu, X. Deng, K. Liu, W. Cai, C. Fu, Integr. Ferroelectr. **150**, 66 (2014).

[42] Y. C. Lee, T. K. Lee, J. H. Jan, J. Eur. Ceram. Soc. **31**, 3145 (2011).

[43] L. Ben, D. C. Sinclair, Appl. Phys. Lett. **98**, 5 (2011).

---

*Corresponding authors: ramzan.karim@giki.edu.pk;
ramzan1109@gmail.com;
khurram@giki.edu.pk